Electronic Supplementary Material (ESI) for Materials Advances.

Fluorine-free synthesized Tantalum carbide (Ta_2C Mxene) as an Efficient Electrocatalyst for Water Reduction and Nitro compound reduction

Aathilingam Vijayaprabhakaran[a,b], Murugavel Kathiresan[a,b]*

[a] Academy of Scientific and Innovative Research (AcSIR), Ghaziabad- 201002, India.

[b] Electro organic and Materials Electrochemistry Division, CSIR-CECRI, Karaikudi, 630003, Tamil Nadu, India, Email: kathiresan@cecri.res.in

1. Experimental parameters

1.1 Hydrogen Evolution Reaction study

The electrochemical investigations and CV studies were conducted in a standard three-electrode setup using Ag/AgCl (3M KCl) as the reference electrode (separated by a salt bridge), platinum sheet as the counter electrode, and modified glassy carbon as a working electrode. The studies were performed in an AUTOLAB Electrochemical workstation operated by Nova 2.1 software. The catalyst was made into a (5 mg in 1 mL) were dispersed into a solution containing ethanol: water in a ratio of (700μL:250μL) respectively. 50 μL of Nafion binder was added to the mixture further to drop casting over glassy carbon (10 μL) dry to overnight at room temperature. The hydrogen evolution reaction (HER) was investigated by linear sweep voltammetry at a scan rate of 2 mV/s in 0.5 M H_2SO_4. The reference electrode was calibrated versus the reversible hydrogen electrode using the following formula.

$E_{RHE} = E_{Ag/AgCl} + E_{0\ Ag/AgCl} + 0.0591 * pH.$

1.2 Electrochemical *p*-Nitrophenol reduction (galvanostatic electrolysis)

The preliminary electrochemical LSV studies were conducted same three-electrode setup using a modified glassy carbon electrode as a working electrode at a scan rate of 50 mV s^{-1} in 1M KOH. The galvanostatic electrolysis was carried out on a two-compartment electrolysis cell separated by a Nafion-324 membrane at room temperature. At the end of electrolysis, the obtained residue was acidified with 1 N H_2SO_4 until pH 6, and the organic products were extracted using ethyl acetate. The organic layer was then collected, washed with water, brine, and dried over anhydrous sodium sulfate, filtered, and evaporated. The desired product was confirmed by H^1 and C^{13} NMR spectroscopy.

1.3 Nitro compounds reduction reaction

The reduction was carried out in the presence of $NaBH_4$ as a reducing agent, and all three aromatic nitro compounds (4-NP, DNP, and TNP) were reduced catalytically. To start the reduction process, at 1 mg of Ta_2C nanoparticles were placed in a quartz cuvette containing 10 ml of 216 μM 4-Nitrophenol (3 mg in 100 mL) similar to other nitro compounds (163 μM, 131 μM) and 240 mg of $NaBH_4$. UV-visible spectroscopy was used to monitor the transformation of 4-nitrophenol (4-NP) into 4-aminophenol (4-AP) at room temperature.

2. Characterisation

2.1 EDAX spectrum

Commercial sample elemental composition: Ta_2AlC (purity: 99.9%) MAX phase

Ta – 90.3%; Al – 6.7%; C – 2.9%; O – 0.03%; B – 0.02%; Sn – 0.01% and Fe – 0.03%

Metals percentage	Ta	Al	C	O	K
Ta_2C-E (FESEM)	71	-	5.8	17.2	6
Ta_2C-E (SEM)	70	-	6.5	16	7.5

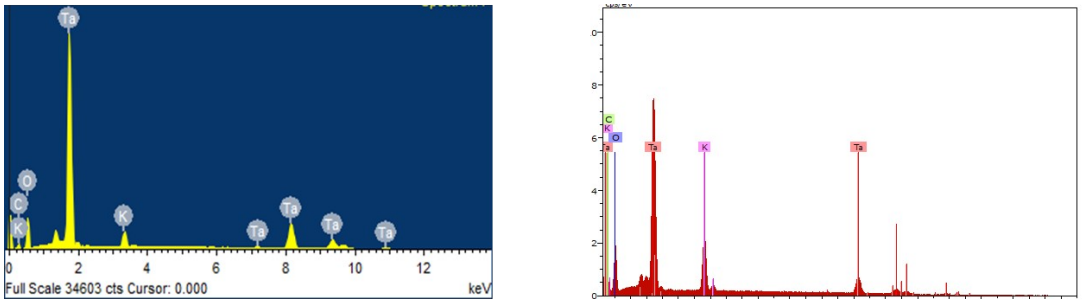

a) Ta_2C-E MXene (FESEM) **b) Ta_2C-E MXene (SEM)**

Figure S1. EDAX spectrum of a) Ta_2C-E MXene (FESEM) and Ta_2C-E MXene (SEM).

2.2 XPS spectrum

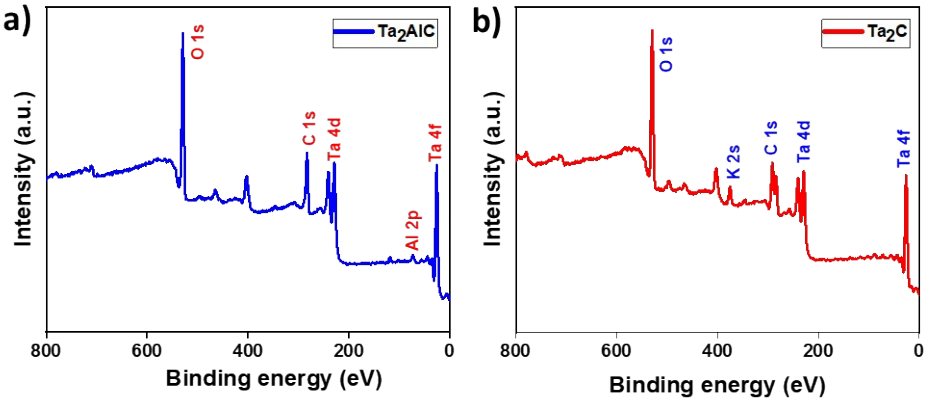

Figure S2 XPS survey spectrum of Ta_2AlC and Ta_2C-E.

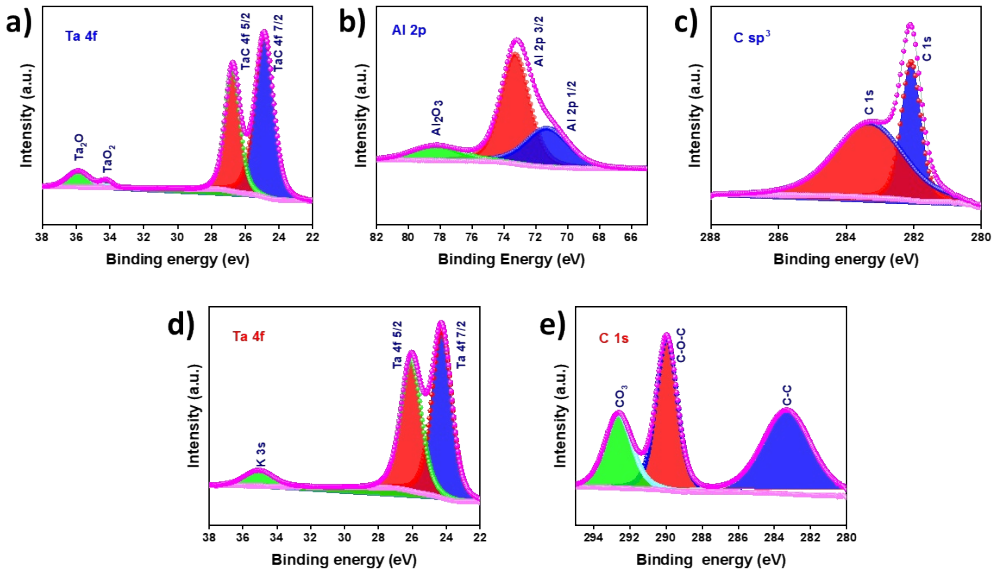

Figure S3 Deconvoluted XPS spectrum of a) Ta 4f, b) Al 2p, c) C 1s of Ta_2AlC and d) Ta 4f, and e) C 1s of Ta_2C-E.

2.3 SEM images

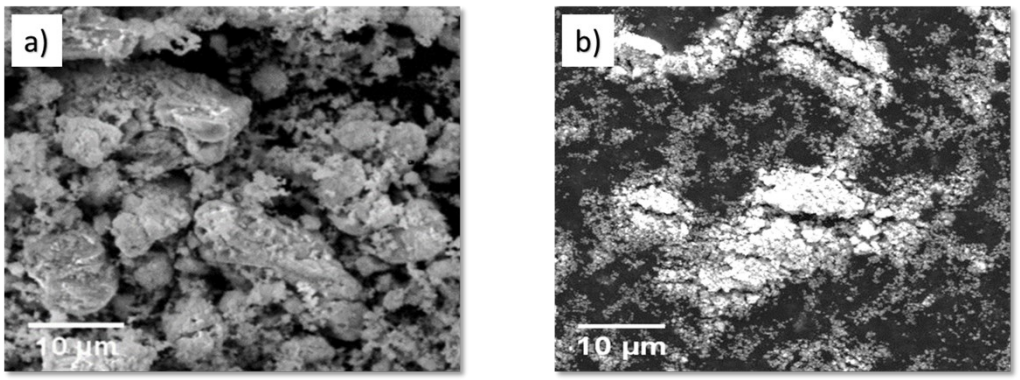

Figure S4 SEM images of Ta_2C-E before (a) and after (b) HER catalytic activity.

2.4 Electrochemical 4-NP reduction

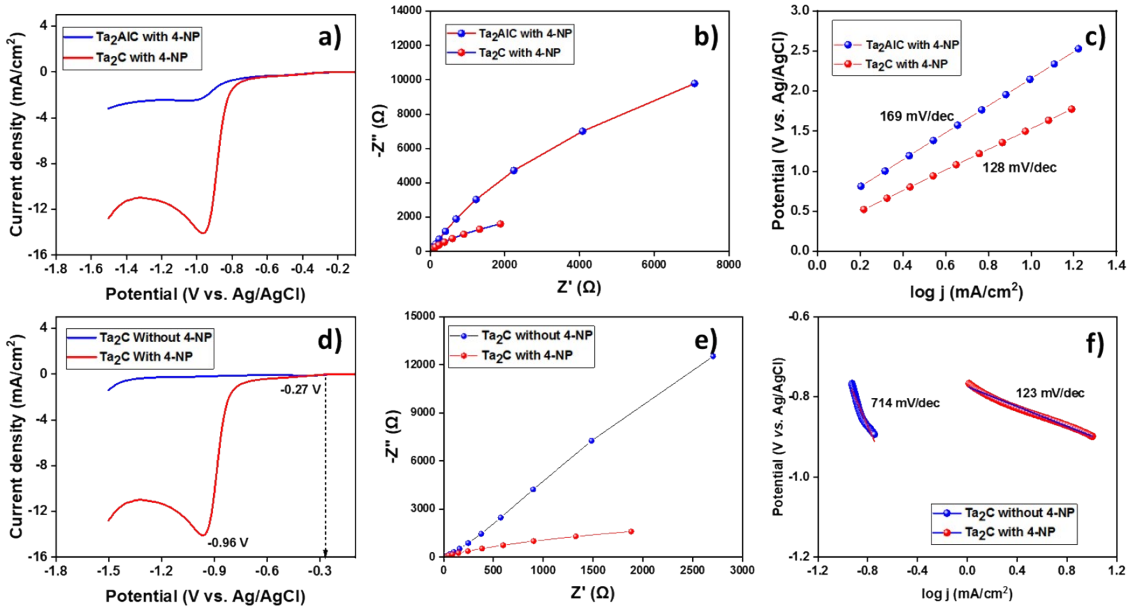

Figure S5 a) LSV of Ta_2C and MAX phase with 4-NP, b) corresponding EIS spectrum, and c) corresponding Tafel plot. d) LSV of Ta_2C-E with and without 4-NP, e) corresponding EIS spectrum, and f) corresponding Tafel plot.

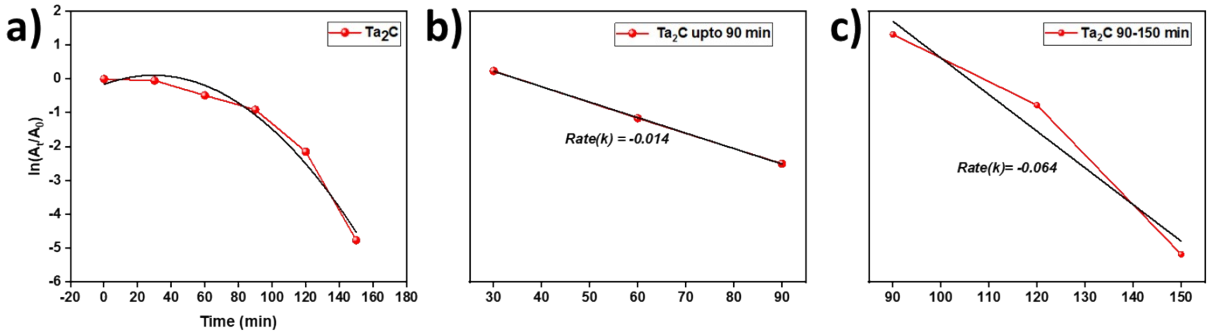

Figure S6. Plots of _ln(At/A0) *vs.* time over samples at each 30 mins derived from Figure 8 d UV-vis absorption spectra revealing the reduction process

2.5 NMR spectrum

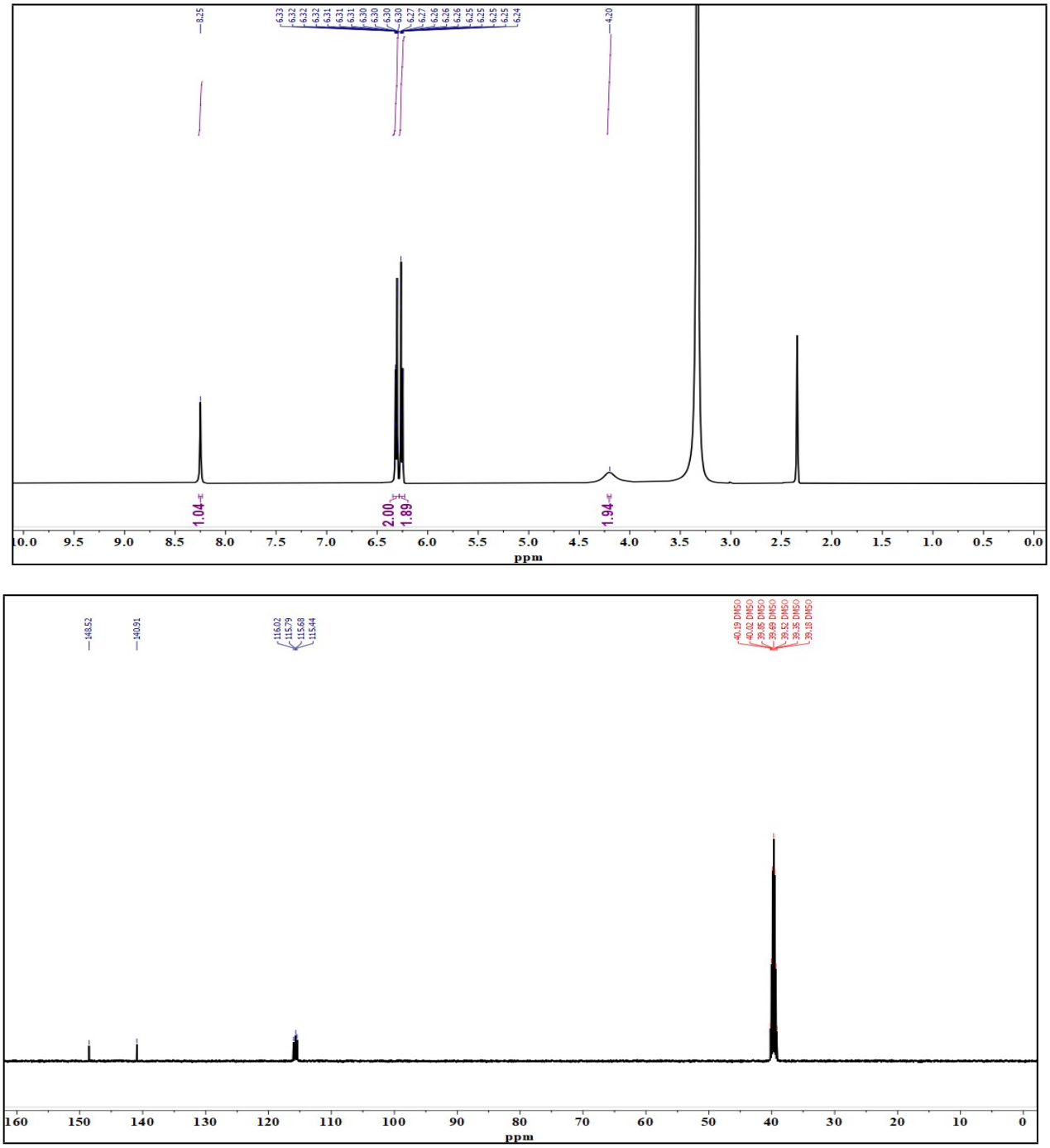

Figure S7 a) H^1 NMR spectrum of *p*-aminophenol and b) C^{13} NMR spectrum of *p*-aminophenol

^{1}H NMR (500 MHz, DMSO-d_6) δ 8.25 (s, 1H), 6.34 – 6.28 (m, 2H), 6.28 – 6.23 (m, 2H), 4.20 (s, 2H). ^{13}C NMR (126 MHz, DMSO-d_6) δ 148.52, 140.91, 116.02, 115.79, 115.68, 115.44, 40.19, 40.02, 39.85, 39.69, 39.52, 39.35, 39.18.

2.6 UV analysis studies

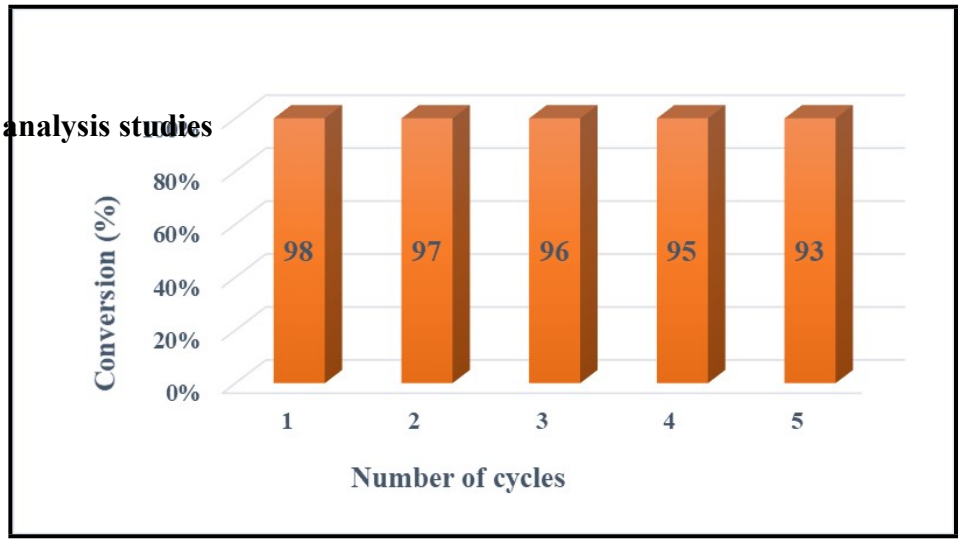

Figure S8 UV-vis absorption results of the reduction process of 5 mL 4-nitrophenol (0.216 mM) with 1 mg of Ta_2C a) recyclability test for 5 consecutive cycles.

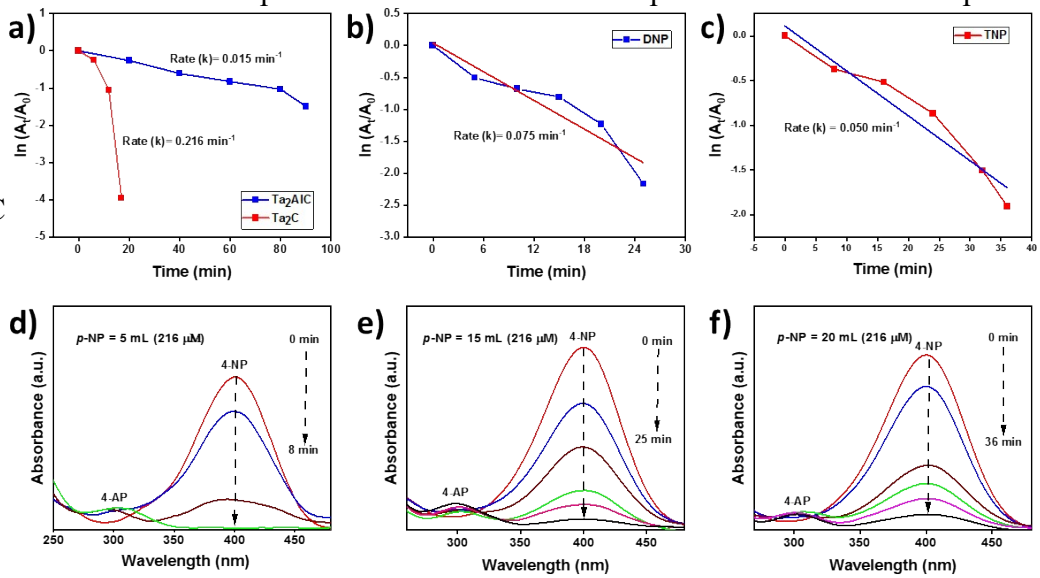

Figure S9 UV-vis absorption spectra reduction with 1 mg of Ta_2C. a-c) plot of $ln(A_t/A_0)$ with Ta_2AlC and Ta_2C-E for the reduction of a) 4-NP, b) DNP, and c) TNP. d-f) UV-vis absorption spectra of the reduction process of d) 5 mL, e) 15 mL, and f) 20 mL of *p*-nitrophenol (216 mM) with 1 mg of Ta_2C.

The kinetic equation for the reduction, which has the following textual form, can be used to determine the apparent rate constant.

$ln(C_t/C_0)$ or $ln(A_t/A_0) = kt$

Where A_t = the absorbance of 4-NP at time t and A_0 = the absorbance of 4-NP at time 0.

The reduction reaction of 4-NP to 4-AP satisfies the pseudo-first-order kinetic equation. The rate constant (k) was determined from the linear plots of ln (A_t/A_0) versus reduction time in minutes.

Hence the reaction rate constant for 4-NP reduction was calculated from the plot of ln (A_t/A_0) Vs time and was found to be 21.6 x 10^{-2} min^{-1} which indicates faster kinetics than MAX phase (1.5 x 10^{-2} min^{-1}) shown in **Fig S8 (a)**. Table 1 shows a comparison of the catalytic performance of various 2D layered catalysts towards the reduction of 4-NP reduction. Further, Ta_2C MXene was tested for its efficacy in converting other toxic pollutants (nitro compounds) such as 2,4-dinitrophenol and 2,4,6-trinitrophenol. The complete DNP reduction occur at 25 min further the kinetic rate constant DNP reduction with Ta_2C was derived from plot 7.5 x 10^{-2} min^{-1} given in **Fig.S8 (b)** Similar that TNP complete reduction occur at 36 min further the kinetic rate constant derived from the similar way we observed 5.0 x 10^{-2} min^{-1} given in **Fig.S8 (c)**.[1]

Table S1 Comparison of electro catalytic activity of HER recently reported MXene based catalyst.

Catalyst	Electrolyte medium	Over potential (mV)	Tafel slope mV/dec	Reference
Mo_2CT_x:Co	1 N H_2SO_4	250	-	2
Mo_2CT_x	0.5 M H_2SO_4	305	74	3
Mo_2TiAlC_2	0.5 M H_2SO_4	570	127	4
N−$Ti_3C_2T_x$	0.5 M H_2SO_4	198	92	5
$NiFe_2O_4/Ti_3C_2$	0.5 M KOH	173	112.2	6
mNC-MoC/Ti_3C_2	0.5 M H_2SO_4	159	70.9	7
$Mo_2TiC_2T_x$ – Pt_{SA}	0.5 M H_2SO_4	30	30	8
Ti_3C_2 NFs	0.5 M	169	97	9
$Ti_3C_2T_x$ flakes	H_2SO_4	385	188	
$Ti_3C_2O_x$	0.5 M	190	60.7	10
$Ti_3C_2(OH)_x$	H_2SO_4	217	88.5	
$Ti_3C_2T_x$-450		266	109.8	
Ta_2CS_2-E	1 M	74	66.9	11
Ta_2CS_2	KOH	105	73.7	
$Ta_4C_3T_x$		139	122.9	
Ta_2C-E	0.5 M H_2SO_4	223	75	This work

Reference

1. Y. Chen, C. Yang, X. Huang, L. Li, N. Yu, H. Xie, Z. Zhu, Y. Yuan and L. Zhou, *RSC Adv.*, 2022, **12**, 4836-4842.
2. D. A. Kuznetsov, Z. Chen, P. V. Kumar, A. Tsoukalou, A. Kierzkowska, P. M. Abdala, O. V. Safonova, A. Fedorov and C. R. Müller, *J. Am. Chem. Soc.*, 2019, **141**, 17809-17816.
3. Z. W. Seh, K. D. Fredrickson, B. Anasori, J. Kibsgaard, A. L. Strickler, M. R. Lukatskaya, Y. Gogotsi, T. F. Jaramillo and A. Vojvodic, *ACS Energy Lett.*, 2016, **1**, 589-594.
4. K. P. Akshay Kumar, O. Alduhaish and M. Pumera, *Electrochem. Commun.*, 2021, **125**, 106977.
5. T. A. Le, Q. V. Bui, N. Q. Tran, Y. Cho, Y. Hong, Y. Kawazoe and H. Lee, *ACS Sustainable Chem. Eng.*, 2019, **7**, 16879-16888.
6. P. V. Shinde, P. Mane, B. Chakraborty and C. Sekhar Rout, *J. Colloid Interface Sci.*, 2021, **602**, 232-241.
7. Y. Tang, C. Yang, Y. Xie, Y. Kang, W. Que, J. Henzie and Y. Yamauchi, *ACS Sustainable Chem. Eng.*, 2023, **11**, 168-176.
8. J. Zhang, Y. Zhao, X. Guo, C. Chen, C.-L. Dong, R.-S. Liu, C.-P. Han, Y. Li, Y. Gogotsi and G. Wang, *Nat. Catal.*, 2018, **1**, 985-992.
9. W. Yuan, L. Cheng, Y. An, H. Wu, N. Yao, X. Fan and X. Guo, *ACS Sustainable Chem. Eng.*, 2018, **6**, 8976-8982.
10. Y. Jiang, T. Sun, X. Xie, W. Jiang, J. Li, B. Tian and C. Su, *ChemSusChem*, 2019, **12**, 1368-1373.
11. T. Wu, X. Pang, S. Zhao, S. Xu, Z. Liu, Y. Li and F. Huang, *Small Struct.*, 2022, **3**, 2100206.